Controlled release of vascular endothelial growth factor from spray-dried alginate microparticles in collagen-hydroxyapatite scaffolds for promoting vascularization and bone repair.

AUTHOR(S)

Elaine Quinlan, Adolfo López-Noriega, Emmet M. Thompson, Alan Hibbitts, Sally-Ann Cryan, Fergal O'Brien

Controlled release of vascular endothelial growth factor from spray-dried alginate microparticles in collagen-hydroxyapatite scaffolds for promoting vascularisation and bone repair

E. Quinlan[1,3,4], A. López-Noriega[1,2,3,4], E. Thompson[1,3,4], A. Hibbitts[1,3,4], S-A. Cryan[1,2,3] and F. J. O'Brien[1,3,4*]

[1]Tissue Engineering Research Group, Dept. of Anatomy, Royal College of Surgeons in Ireland, 123 St. Stephen's Green, Dublin 2, Ireland

[2]School of Pharmacy, Royal College of Surgeons in Ireland, 123 St. Stephen's Green, Dublin 2, Ireland

[3]Trinity Centre for Bioengineering, Trinity College Dublin, Dublin 2, Ireland

[4]Advanced Materials and BioEngineering Research (AMBER) Centre, RCSI & TCD, Dublin 2, Ireland

*Corresponding author: fjobrien@rcsi.ie; +35314022149

Abstract

A major limitation with current tissue engineering approaches is creating functionally vascularised constructs that can successfully integrate with the host; this often leads to implant failure due to avascular necrosis. In order to overcome this, the objective of the present work was to develop a method to incorporate growth-factor-eluting alginate microparticles (MPs) into freezedried collagen-based scaffolds. A collagen hydroxyapatite (CHA) scaffold, previously optimized for bone regeneration, was functionalised for the sustained delivery of an angiogenic growth factor (vascular endothelial growth factor-VEGF) with the aim of facilitating angiogenesis and enhancing bone regeneration. VEGF was initially encapsulated in alginate MPs by spray-drying producing particles of <10 μm in diameter. This process was found to effectively encapsulate and control VEGF release while maintaining its stability and bioactivity post-processing. These VEGF-MPs were then incorporated into CHA scaffolds leading to homogenous distribution throughout the interconnected scaffold pore structure. The scaffolds were capable of sustained release of bioactive VEGF for up to 35 days which was proficient at increasing tubule formation by endothelial cells *in vitro*. When implanted *in vivo* in a rat calvarial defect model this scaffold enhanced vessel formation resulting in increased bone regeneration compared to an empty defect and VEGF-free scaffold. This biologically functionalised scaffold, composed entirely of natural-based materials, may offer an ideal platform to promote angiogenesis and tissue regeneration.

Keywords

Polymeric alginate microparticles; vascular endothelial growth factor; angiogenesis; osteogenesis; collagen scaffolds; tissue engineering; spray-drying

1. Introduction

More than 2.2 million orthopaedic procedures requiring bone grafts are conducted worldwide annually, making bone the second most commonly transplanted tissue next to blood (Marino and Ziran 2010). Due to limitations of current therapeutic approaches, the engineering and regeneration of bone via tissue engineered (TE) scaffolds is being explored extensively. A wide range of collagen-based scaffolds exist for tissue engineering (Wahl and Czernuszka 2006; Swetha *et al.* 2010) a number of which have been developed and optimised in our research laboratory for bone repair to include synthetic ceramics and natural polymers (Cunniffe *et al.* 2010; Haugh *et al.* 2010; Keogh *et al.* 2010). These scaffolds provide a suitable porous structure and substrate for tissue growth by mimicking the natural extracellular matrix (ECM). One of the biggest challenges faced in the TE field is promoting the growth of vasculature within engineered tissues to enable sufficient engraftment and integration within the host (Novosel *et al.* 2011). The diffusion distance for nutrients and oxygen implicit to cell survival is limited (150-200μm) and this can lead to necrosis in the centre of the supportive scaffolds designed, for example, for bone repair. Traditional methods of initiating angiogenesis and osteogenesis include delivering recombinant human (Rh) growth factors (GFs) such as Vascular Endothelial Growth Factor (VEGF) and Bone Morphogenetic Proteins (BMP) (Lieberman *et al.* 2002) as well as direct delivery of genes encoding for these GFs (Lu *et al.* 2013). Specifically, delivery of VEGF represents a particularly promising means of enhancing angiogenesis and osteogenesis due to the fact that this protein has the ability to increase vascular network formation and vascular permeability (Stacker and Achen 1999) resulting in increased blood flow and access of the defect site to progenitor cells. Additionally, VEGF is also an inducer of osteoblast differentiation serving to promote cell recruitment acting as a chemo attractant for mesenchymal stem cells (MSCs), osteoblasts and osteogenic cells suggesting a role for VEGF in coupling angiogenesis and

osteogenesis (Mayr-Wohlfart *et al.* 2002; Patel *et al.* 2008). However, current GF delivery approaches for VEGF and other GFs are often associated with limited success due to the uncontrolled manner in which proteins are released, short half-life, high doses required to reach the target tissue, potential safety concerns within a clinical setting and high costs (Epstein 2011; Lu *et al.* 2013).

In an attempt to overcome these issues, several scaffold-based systems either naturally or synthetically derived have been developed to deliver GFs to the target sites. The most common approach consists of GFs directly interspersed within a scaffold through soak loading. One example is Medtronic's INFUSE®, a bone graft substitute consisting of an absorbable collagen sponge soaked with recombinant BMP-2. This product, although approved by the US Food and Drug Administration (FDA), has been associated with side effects and complications such as heterotopic bone growth or bone overgrowth as well as haematomas in soft tissue, para-implant bone resorption and osteolysis. This occurs as a result of BMP-2 leakage into other areas of the body due to the uncontrolled manner in which the GF is released (Epstein 2011). These shortcomings demonstrate the need for alternative drug delivery strategies capable of controlling growth factor delivery to particular sites. This has led to the emergence of scaffolds integrated with GF delivery devices in the form of polymer microparticles which serve to protect the GF whilst controlling its release (Richardson *et al.* 2001; Chen and Mooney 2003). The scientific literature describes an array of microparticle engineering methodologies for encapsulating drugs in a variety of matrix materials including emulsion dispersion (Borselli *et al.* 2010), ionotropic pregelation (Reis *et al.* 2006) and spray drying (Schoubben *et al.* 2010). However, emulsion dispersion and ionotropic gelation possess limitations in that they are difficult to scale up and typically involve the use of toxic organic solvents. Spray-drying is a rapid method to produce calcium alginate microparticles with few processing parameters compared to other techniques making

it suitable for industrial scale up (Sivadas *et al.* 2008; Schoubben *et al.* 2010). In the current study, the encapsulation of VEGF in spraydried microparticles produced from the natural polymer alginate was investigated. Alginate is biodegradable, biocompatible and categorised in the generally regarded as safe (GRAS) classification by the FDA (George and Abraham 2006). Furthermore, it has many possible applications in the area of drug delivery and controlled release (Lee and Mooney 2012).

These spray-dried microparticles were incorporated into scaffolds with properties optimised specifically to promote cell infiltration and tissue formation. Recent work in our laboratory has led to the development of a highly porous collagen-hydroxyapatite (CHA) scaffold that combines biodegradability and biocompatibility characteristics of collagen with the naturally occurring and osteoconductive bone mineral hydroxyapatite (Gleeson *et al.* 2010). Previously this has been shown to facilitate bone regeneration in two pre-clinical models: rat calvaria (Gleeson *et al.* 2010) and rabbit radii (Lyons *et al.* 2014). The aim of the current study was thus to enhance the regenerative capacity of this scaffold through the incorporation of therapeutic GFs. Specifically; the scaffold was functionalised with VEGF-releasing alginate microparticles in an attempt to engineer a material capable of localising and sustaining the release of VEGF over extended periods, in order to promote vascular ingrowth and enhance bone formation. Herein, we describe the *in vitro* development and characterisation of this functionalised CHA scaffold through the combination of the above materials with the ultimate aim of assessing the functionality and bioactivity of the scaffold *in vivo*.

2. Materials and Methods

2.1 Preparation of VEGF-loaded alginate microparticles

Alginate microparticles (MPs) were prepared using low viscosity alginic acid sodium salt from *Macrocystis pyrifera* (Sigma, Ireland) by a spray-drying method. Fluorescently labelled Bovine Serum Albumin (BSA) with a Fluorescein Isothiocyanate tag (FITC) (Sigma, Ireland) was initially incorporated as a model protein cargo as previously described (Sivadas *et al.* 2008) to determine the protein-MP distribution within the scaffolds. RhVEGF165 (R&D Systems, UK) was similarly incorporated into alginate MPs. A 0.5% w/v alginate feed solution was mixed with VEGF (1µg/mg) and spray-dried (Buchi Mini Spray-Dryer B290) according to the following drying parameters: compressed air 5-8 bar, air flow rate 400-600L/hr, inlet temperature 140 °C, aspirator at 80% of maximum capacity, and pump flow rate at 15%. These were based on previously established parameters for fabricating particles of an appropriate size range for the intended application (Sivadas *et al.* 2008). MPs were obtained in powder-form from the spray-drier and subsequently crosslinked. With this purpose, MPs were suspended in acetonitrile to disperse them under sonication (Schoubben *et al.* 2010) and the suspension was poured into 1.2% (w/v) calcium chloride solution under magnetic stirring (10 min). The particles were filtered on 0.45 µm nylon filter paper, washed twice with distilled water to remove the solvent and dried at room temperature overnight. The recovered MPs were stored at 4 ºC in a dessicator until further use.

2.1.1 Microparticle yield and size

The mass yield of product after spray-drying and crosslinking was determined according to the below equation.

Yield (%) = mass of MPs post spraydrying (g)/ (polymer + protein in spraydryer (g) x 100

The mean particle size and size distribution of the MPs were determined by dynamic light scattering (DLS) with a Malvern MasterSizer Sirocco 2000 by suspending the particles in distilled water prior to analysis. Size and surface morphology of the VEGF-MPs was

characterized using a scanning electron microscope (SMU SEM, Japan) and an optical microscope (Olympus CX-41). Prior to SEM observation, the particles were mounted on metallic studs coated with thermoplastic carbon adhesive and later sputtered with gold.

2.1.2 VEGF loading and encapsulation efficiency

To determine the content of VEGF encapsulated in the polymer, 5 mg of dried and crosslinked VEGF-MPs were dissolved in 10 mLs of 0.1 M sodium citrate under magnetic stirring for 30 min and the VEGF content analysed by ELISA using a rhVEGF DuoSet® ELISA Development kit (R&D Systems, UK) according to the manufacturer's instructions.

Drug loading and encapsulation efficiency were defined as:

Loading efficiency, LE (%) = encapsulated drug/microparticle weight,

Theoretical loading efficiency, TLE (%) = drug used for encapsulation/ (protein + polymer used for encapsulation),

Encapsulation efficiency, EE (%) = LE/TLE

2.1.3 In vitro growth factor release kinetics from microparticles

In order to examine VEGF release kinetics from the alginate MPs, 20 mg of VEGF-MPs were dispersed in 2 mLs of Dulbecco's Phosphate Buffered Saline (PBS; 140mM NaCl, 1.5mM KHPO4, 8.1mM NaHPO4, 2.7mM KCl; Sigma-Aldrich, Germany) placed in a waterbath and shaken at 37 ºC. The release medium was removed following centrifugation and replaced by fresh PBS at the following timepoints for analysis; 4 h, day 1, 3, 7, 14, 21 and 28. VEGF in the release media was quantified using the rhVEGF ELISA above according to the manufacturer's instructions.

2.2 In vitro bioactivity of VEGF released from microparticles

2.2.1 Cell culture

To assess the bioactivity of VEGF released from alginate MPs, Human Umbilical Vein Endothelial Cells (HUVECs) were cultured in complete endothelial media (EGM-2 BulletKit, Lonza, UK) in T175 flasks under standard culture conditions (37 ^{o}C, 5% CO_2) until they reached 90% confluency. Media was replaced every 3-4 days. Cells were passaged every 5-6 days. A confluent flask was rinsed with 10 ml of pre-warmed PBS to remove any trace of media and trypsinised (0.25% EDTA/Trypsin (Sigma-Aldrich, Germany). Flasks were returned to the flow hood where 4-5 ml of medium was added to deactivate the trypsin and the cells were counted using a haemocytometer. The collected suspension was then centrifuged (5000rpm for 5 min), the supernatant was discarded and the pellet was resuspended in growth media without VEGF and seeded according to the below parameters.

2.2.2 Tubule formation in response to released VEGF

To examine the ability of VEGF released from VEGF-MPs to enhance angiogenesis, Growth Factor Reduced Matrigel™ (BD Biosciences, UK), a basement membrane matrix commonly used to observe *in vitro* angiogenesis, was placed in a 48 well plate (120 µL/well). The release media (containing VEGF) was diluted to achieve a VEGF concentration previously shown to enhance tubule formation (50 ng/mL) *in vitro* in a similar assay (Suehiro *et al.* 2010). HUVECs were plated at $3x10^4$ per well and placed in an incubator for 20 min after which time different cell culture media was added including; 1 mL of endothelial medium without the VEGF supplement in all cases, endothelial media containing VEGF previously released from VEGF-MPs (for 4 h) and diluted to 50 ng/mL or non encapsulated VEGF aliquoted from fresh VEGF stock solution at the same concentration used as a bioactivity benchmark control. Phase contrast light microscopy images of the cells at 10x magnification were captured at 6 h, 12 h and 24 h post-seeding with an in-situ camera (LEICA DFC420C) using a Leica DMIL microscope (Leica Microsystems, Switzerland). Image J software (Abramoff *et al.* 2004) (National Institutes of Health) was used to determine the total tubule

length of each tube in each image (5 images/well) and the average cumulative length per well was calculated in response to the various culture conditions used as a surrogate marker of angiogenesis.

2.3 Fabrication and characterisation of CHA and functionalised CHA scaffolds

Having established the method of VEGF-MP preparation and maintenance of VEGF bioactivity, a collagen-hydroxyapatite (CHA) scaffold was fabricated using a patented freeze-drying process developed by the RCSI Tissue Engineering Research Group (O'Brien 2008; Gleeson *et al.* 2010; Lyons *et al.* 2014). Briefly, collagen (Collagen Matrix, Inc, New Jersey) slurries were produced by the homogenization of 1.8 g of fibrillar collagen within 320 mL of a 0.5 M acetic acid solution. Slurries were homogenized in a reaction vessel at 4 °C using an overhead blender. In parallel, 3.6 g of hydroxyapatite (HA) particles with a size 3-8 μm (Plasma-Biotal Ltd) were suspended in 40 mL of a 0.5 M acetic acid solution. The final CHA slurry (200% HA/collagen weight ratio) was produced by the addition, in aliquots, of the HA/acetic acid suspension to the initial collagen slurry during the homogenization process. The slurry was degassed under a vacuum to remove air bubbles and subsequently 9 mL was pippetted into a stainless steel pan (45 x 45 mm, grade 304 SS). The tray was placed into a freeze-dryer and cooled to -10 °C at a constant rate of 0.9 ºC/min. Once freezing was complete, the ice crystals were removed by sublimation for 17 h at 200 mTorr. The resulting materials were cut with a punch into 6.5 mm diameter discs with a depth of 3-4 mm.

In order to incorporate the MPs into the scaffold for the formation of a functionalised CHA scaffold they were suspended in water for achieving three difference concentrations within the CHA slurry; 0 (control scaffolds), 0.5, 1.1 and 2.2% w/v (weight of microparticles/volume of slurry) equating to 0, 1.5, 3.3 and 6.6 μg of protein. They were then dispersed with the CHA slurry and freeze-dried as above. This fabrication process is the subject of a patent filing (O'Brien *et al.* 2012). Blank and BSA-FITC loaded MPs were

initially incorporated to establish the maximum MP loading achievable so as not to affect the porosity and mechanical properties of the scaffold. VEGF-MPs were subsequently incorporated into the slurry at the maximum MP loading capacity, determined to be 0.5% w/v of CHA slurry, based on scaffold characterisation studies, according to results that are shown in the supplementary information. This VEGF-releasing scaffold will be denoted VEGF-MP scaffold in the remainder of the manuscript. Scaffolds were crosslinked under an ultra-violet (subtype C, 365 nm λ) lamp for 15 mins and were turned half way through to enhance the mechanical and enzymatic resistance properties of the materials (Weadock *et al.* 1995; Weadock *et al.* 1996). Scaffolds were subsequently sterilised under the UV lamp (254 nm λ).

Confocal Laser Scanning Microscopy using a LSM 510 Axio plan 2 upright confocal microscope (Carl Zeiss, Germany) was used for assessing the distribution of flourescently labelled MPs in different layers and regions of the BSA-FITC loaded MP scaffolds and carrying out 3-dimensional reconstructions from these images Scaffolds were cut and mounted onto metallic studs with the help of carbon-based glue and sputtered with gold and SEM images were captured at a voltage of 5 kV using secondary electron mode, taken at a working distance between 12-18 mm. Both the surface and the cross-section of the MP scaffolds were examined.

2.4 Analysis of VEGF release and bioactivity from VEGF-MP scaffolds

In order to examine VEGF bioactivity following scaffold fabrication, protein was released from VEGF-MP scaffolds by placing 6 mm scaffolds in 2 mLs of PBS. At set timepoints; 4 hrs, day 1, 3, 7, 14, 21, 28 and 35, buffer was removed and a fresh aliquot of PBS was added to the scaffold. ELISA was used for protein quantification as described above. To examine the ability of VEGF released from scaffolds to enhance angiogenesis, Matrigel™ was similarly employed as described for VEGF-MPs (section 2.2). Endothelial media containing

VEGF released from VEGF-MP scaffolds (for 4 h) and diluted to 50 ng/mL instead of protein released from VEGF-MPs, was used.

2.5 Effect of functionalised VEGF-MP scaffolds on *in vivo* bone formation and vascularisation

2.5.1 Surgical procedure

In vivo analysis was conducted in accordance with protocols approved by the Research Ethics Committee of the Royal College of Surgeons in Ireland and an animal license was granted by the Irish Government Department of Health (Ref. B100/4416). A total of 24 young adult (ca. 12 weeks) male Wistar rats (mean weight 375 g, range 360-395 g) were divided into 3 groups: 1) empty defect (*n*=8) denoted 'empty defect' 2) CHA scaffold alone (no MPs or VEGF) (*n*=8) denoted 'empty scaffold', 3) CHA scaffold containing alginate MPs encapsulating VEGF (*n*=8) denoted 'VEGF-MP scaffold'. General anaesthesia, the creation of the 7-mm-diameter critical-size cranial defect, the placement of the composite materials in the defect site, and postoperative animal care were performed using established methods in our lab (Lyons *et al.* 2010; Quinlan *et al.* 2015). In all cases a trephine was used to create a transosseous defect, confirmed by identification of the dura at surgery which remained intact. The rehydrated scaffold was implanted into the defect, the periosteum kept intact and oversewn with 3/0 absorbable monofilament suture (Ethicon, NJ, USA) and the skin closed with skin glue (3M™ Vetbond™ Tissue Adhesive (n-butyl cyanoacrylate)). All rats were housed in the Biomedical Research Facility at the Royal College of Surgeons in Ireland, Dublin 2, Ireland. At 8 weeks post-implantation, the animals were euthanized by CO_2 asphyxiation, a 20 x 20 mm segment of calvarium containing the defect was resected using a dental saw (Dentalfarm, Torino, Italy) and the explants retrieved were stored in 10% formalin for 4 days and then transferred to PBS prior to analysis.

2.5.2 Immunohistochemical staining

The endothelial cell marker platelet endothelial cell adhesion marker (PECAM/CD31) was analysed to observe the ability of VEGF released from the scaffolds to promote vessel formation as it is highly expressed in endothelium (Zocchi *et al.* 1996; Norrby and Ridell 2003). CD31 is a commonly used endothelial marker for quantifying angiogenesis by calculation of Microvessel Density (MVD) (Norrby and Ridell 2003). For quantification, cross-sections (7 μm) of decalcified, paraffin embedded tissue (described below) representing the peripheral and central regions of the scaffold (8 scaffolds per group with n=6 sections analysed per scaffold) were deparaffinized, rinsed in PBS, surrounded by a PAP pen and incubated in blocking buffer consisting of horse serum and 1% BSA in PBS (Vectastain Elite Kit, Vector laboratories, CA, USA) for 1 h. The specimens were washed in PBS/Tween 20 and incubated in mouse anti-rat primary CD31 antibody (BD Biosciences, UK) at a dilution of 1:650 in 1% BSA in PBS for 1h at room temperature and then mounted with Vectashield (Vectastain Elite Kit). Images were taken with a fluorescence microscope (Olympus IX51-AnalySIS imaging system) where FITC-labelled ECs in sections were visualised. Nuclei were stained with DAPI to identify the presence of vessel forming ECs. Vessel area is then measured using the DAPI images to select for vessel forming ECs subtracing any staining due to the presence of scaffold. Vessel area (average of the total area covered by red stained vessels in the sections) and density (total number of vessels found in the biomaterial) were quantified using ImageJ software.

2.5.3 Microcomputed tomography analysis

The three dimensional (3D) structure of the new bone produced within the cranial defect was analysed using micro computed tomography (microCT). Scans were performed on a Scanco Medical 40 MicroCT system (Scanco Medical, Bassersdorf, Switzerland) with 70 kVP Xray source and 112 μA (resolution of ~12μm). 3D reconstruction was performed using the

standard Scanco software package and a threshold of 140 in a scale from 0–1000. Volume of interest (VOI) was defined to analyze a 6 mm defect region to assess healing in the centre of the defect excluding any old bone at the defect edges. Repair was expressed as percentage bone within the defect area.

2.5.4 Histological analysis

Along with microCT, both qualitative and quantitative histological examinations were performed on explants in order to assess the levels of bone and vascular formation throughout the scaffold following implantation for 8 weeks. After microCT analysis, the implants were decalcified for 3-4 weeks depending on the level of mineralisation using Ethylenediaminetetraacetic acid (EDTA) 14% (w/v) at pH 7.4. The specimens were bisected, wax embedded, sectioned (7 µm) and stained with Haematoxylin and Eosin (H&E). Images were taken using transmitted light and epifluorescence microscopic visualisation (Nikon Microscope Eclipse 90i, Nikon Instruments Europe, The Netherlands). The defect margin was identified and quantitative histomorphometric analysis was carried out using a blind scoring method to quantify the healing response from the H&E-stained samples by calculating the average area of bone nucleation sites (stained pink) formed in cross-sections representing the peripheral and central regions of the scaffold using ImageJ (8 scaffolds/group with n=6 sections analysed/scaffold).

2.6 Statistical analysis

Results are expressed as mean ± standard error of the mean (SEM). Statistics were carried out using GraphPad Prism software using a general linear model ANOVA followed by Tukey and Bonferroni post hoc analysis unless otherwise stated. The sample size was n=3 for *in vitro* and n=8 for *in vivo* studies where $p \leq 0.05$ values were considered statistically significant.

3. Results

3.1 VEGF-microparticle characterisation

A process yield after spraydrying of 54 ± 4% was determined for blank alginate and BSA-FITC loaded MPs and 65 ± 4% for VEGF loaded MPs. Scanning electron micrographs of the VEGF-MPs show particles which are irregularly shaped although generally smooth and spherical, features which have previously been described for alginate microparticles fabricated by spraydrying (Bowey *et al.* 2013), with diameters lower than 10 µm in size (Fig. 1A). DLS measurements confirmed these observations, as diameters of the VEGF-MPs were found to be distributed in the range of 1-20 µm with an average size of 3.9µm. Protein encapsulation efficiency of the VEGF loaded alginate MPs was next determined by relating the loading efficiency (0.045%) to the total theoretical loading efficiency (0.1% protein: polymer). The content of encapsulated protein as determined by ELISA was found to be 49 % of the original amount of VEGF incorporated during the fabrication process.

3.2 Analysis of VEGF release and bioactivity from VEGF microparticles

The release profile of VEGF from the MPs, displayed in Figure 1C, was continuous and sustained at high levels for up to 4 days after which time protein release dropped at 7 days. Following this, a decrease in VEGF release was seen thereafter from day 10 where minimum concentrations were recorded until the end of the study. At the end of the study 28% of the protein was released cumulatively. Surprisingly, when the particles were digested at the endpoint of the study they were shown to still contain 20% of the initially incorporated protein.

The ability of the encapsulated VEGF to stimulate the tubule formation potential of HUVECs was determined by culturing ECs with VEGF released from VEGF-MPs and subsequently quantified and diluted to 50 ng/mL. There HUVECs displayed enhanced tubule network

formation (6 h and 12 h) compared to the rhVEGF control (non encapsulated) added to the media at the same concentration. In addition, the ability of encapsulated VEGF to stimulate EC proliferation was also enhanced to a similar extent as the rhVEGF control when compared to cells in the absence of VEGF (see supplementary information).

3.3 Characterisation of MP distribution and pore size of functionalised scaffolds

Confocal microscopy characterisation of scaffolds incorporating BSA-FITC loaded MPs was used to demonstrate the uniform spreading of the MPs throughout different layers within the scaffolds at all MP concentrations incorporated (see supplementary information and Figure 2 A). Scanning electron microscopy images, displayed in Figure 2, corroborated these results, as they demonstrate the homogeneous distribution of the polymer particles through the collagen matrix. The pore diameters of the scaffolds decreased as a function of the increasing concentrations of MPs with pore size significantly highest (100 μm) in scaffolds containing the lowest MP concentration (see supplementary information). Since the optimal range of scaffold pore sizes for bone tissue regeneration is between 100 μm and 135 μm (Murphy and O'Brien 2010), scaffolds with a concentration of microparticles of 0.5% were selected for further studies.

3.4 Analysis of VEGF release and bioactivity from VEGF-MP scaffolds

The kinetics of VEGF eluted from the MPs which were incorporated within the scaffold was next assessed. Similarly to the delivery from the microparticles alone, the total release achieved at the endpoint of the study from the scaffolds was 26% (427 ng) of the initially incorporated VEGF (Fig. 2D). A high burst release of greater than 160 ng VEGF (10% of the total loaded protein) was recorded from the VEGF-MP scaffolds, in contrast to the release kinetics observed from the MPs alone (i.e. not embedded in a scaffold) where no burst release was detected. This was followed by a lower VEGF release at 24 h and a burst again of 7% of

loaded protein at day 4. After 4 days, a slow release of VEGF was sustained until the end of the assay.

Having determined the release kinetics of VEGF from the scaffolds the next step was to examine whether the process of VEGF-MP scaffold preparation had any detrimental effect on VEGF bioactivity. This was shown not be the case and VEGF bioactivity was retained following the various process parameters (Fig. 3A, B). It was observed that ECs cultured with VEGF released from VEGF-MP scaffolds displayed enhanced tubule network formation to a similar extent as rhVEGF added directly to the media at the same concentration compared to cells cultured in the absence of VEGF for 6 h. Regression of the tubules observed between 12 and 24 h is a typical behaviour of these capillary-like structures as previously reported (Kubota *et al.* 1988; McCoy *et al.* 2013).

3.5 Effect of functionalised scaffolds on *in vivo* vascularisation and bone formation

3.5.1 Assessment of the angiogenic effect of VEGF-MP scaffolds

The ability of the scaffolds to promote *in vivo* angiogenesis was evaluated by quantifying immunohistochemically stained endothelial cells (Fig.4A). An observably higher angiogenic response was evident in the VEGF-MP group correlating to a high level of neovascularisation compared to all other groups. Empty scaffolds had no effect on angiogenesis when compared to empty defects. Importantly, in the VEGF-MP group, quantitative analysis revealed a 3-fold increase in the number of *de novo* blood vessels compared with that of the empty defect (Fig. 4C). Furthermore, the VEGF-MP scaffolds led to a 2-fold increase in vessel area compared with the empty defect and a 5-fold increase compared to the empty scaffold (Fig. 4D). In summary, these results demonstrate the ability of VEGF eluted from the functionalised scaffolds to enhance angiogenesis.

3.5.2 Assessment of the osteogenic effect of VEGF-MP scaffolds

Having determined the angiogenic effects of the VEGF-releasing functionalised scaffold, the effects of the scaffold on bone formation were studied by microCT imaging (Fig. 5A) revealing the higher extent of new bone formation in the functionalised scaffolds when compared to the empty defect control (significant) and the empty scaffold (non significant) Fig. 5B). While the empty scaffold group also displayed higher bone volume compared to the empty defect the volume was reduced compared to the VEGF-MP group. To further characterise the levels of healing, H&E staining was carried out on explants after 8 weeks, results of which are shown in Figures 5C and 5D. Overall, less healing was found in the empty defect compared to all other groups. In the empty defect group, the defect space was primarily occupied by busy thin fibrotic tissue (Fig. 5C and high mag image below) and very little bone formation had occurred. In the empty scaffold group bone formation occurred predominantly at the defect edges. Cellular infiltration was seen in all scaffolds with some level of bridging occurring as confirmed in the microCT images of empty defect versus scaffold groups (Fig. 5A). In the defects treated with VEGF-MP scaffolds, enhanced bone regeneration was evident when compared to the CHA scaffold alone and empty defect (high mag images). A much thicker region of bone formation was obvious, with good cell infiltration throughout the construct (Fig. 5C) and high levels of bone bridging. These observations were further confirmed by quantitative histomorphometrical analysis demonstrating the enhanced area of new bone formed resulting from VEGF-MP treatment. This was significantly higher than in the empty defect group as well as the defects treated with non-VEGF eluting empty CHA scaffolds (Fig. 5D). Taken together, these data demonstrate the ability of the VEGF-MP scaffold to promote bone formation *in vivo*.

4. Discussion

The role of scaffolds for bone tissue repair is progressively evolving from simple support materials for cell growth to bioactive matrices which can also deliver pro-regenerative factors

to enhance tissue regeneration. The aim of this study was to deliver VEGF in a controlled and sustained manner from polymer microparticles embedded within a collagen-hydroxyapatite scaffold previously developed for bone regeneration, in order to enhance its therapeutic potential by increasing angiogenesis. The extensive characterization carried out in this study demonstrates that, with the proposed fabrication technique it is possible to create these functionalised scaffolds which were shown to be capable of enhancing blood vessel formation. In addition the VEGF-releasing functionalised scaffold also facilitated increased bone repair in a critically sized rat calvarial defect model.

To the best of our knowledge, the present work describes for the first time the encapsulation of VEGF in alginate using a spraydrying technique and a complex multistep process for the subsequent incorporation of these MPs into a 3D scaffold developed for tissue engineering applications. The spray-drying process was chosen since it is widely used at an industrial level for the manufacture of particulate systems as it enables production of small diameter MPs with high yields and drug encapsulation efficiencies (Hascicek *et al.* 2003). In the present work, the size of VEGF-eluting microparticles were in the range of 1-20μm, in accordance with alginate materials fabricated similarly (Bowey *et al.* 2013). Importantly, VEGF was released at timepoints relevant to its *in vivo* expression profile reported in fracture healing models suggesting the potential of this delivery system to mimic the innate *in vivo* response (Tsiridis *et al.* 2007). Furthermore, the growth factor maintained its bioactivity during the encapsulation process; VEGF released from the MPs was proficient at increasing tubule formation by ECs *in vitro*. Additionally, when compared with non encapsulated, fresh rhVEGF used as positive control, tubule formation was enhanced, probably due to alginate dissolving from particles into the release media which may alter the binding of VEGF to VEGF receptors on ECs thereby prolonging the effects (Peters *et al.* 1998). At the endpoint of the study, MPs were shown to still retain 20% of the originally loaded protein, indicating

physical integrity of VEGF even after 28 days in an aqueous solution. The remainder of the protein may have degraded to a variable extent in the PBS. Taken together, the results confirmed the feasibility of spray-drying as a method of MP fabrication for encapsulation of VEGF. Thus, these VEGF loaded MPs were incorporated into scaffolds in order to enhance their angiogenic capacity. Such scaffolds would possess dual functionality; they would enhance bone regeneration due to the osteoinductive nature of the matrix (Gleeson *et al.* 2010) while providing a physical support for the MPs to release VEGF in the target tissue thereby promoting angiogenesis.

The final fabrication process resulted in scaffolds with mean pore sizes greater than 100 μm – a size range known to facilitate proliferation of osteoblasts and osteogenic differentiation of MSCs (Hulbert *et al.* 1970; O'Brien *et al.* 2005; Byrne *et al.* 2008; Murphy and O'Brien 2010). Furthermore the fabrication process resulted in a homogenous distribution of the MPs throughout the scaffold - a beneficial result which allows controlled spatial delivery of the GF, an effect which can be lost when particles aggregate (Langer 1998). Cumulative release data suggested a controlled release profile from the scaffolds with a high initial burst release followed by a slower release for up to 4 days after which time a steady state sustained VEGF delivery profile was observed. The high burst release is likely a result of protein being released from MPs at first contact with the acidic environment of the CHA slurry prior to freeze-drying. Spraydried MPs typically accumulate their cargo on the outer surfaces (Vehring 2008) and since MPs may partially dissolve in contact with the slurry, the aggregated drug on the outer surface is released in an uncontrolled manner. Although there is little conclusive information regarding the specific VEGF concentration required to elicit an *in vivo* biological response, it has been demonstrated that higher concentrations of VEGF for a period of up to 7 days followed by lower concentrations as well as a distributed pattern of delivery, as achieved with this scaffold, is more effective at permitting neovascularisation

(Stacker and Achen 1999; Street *et al.* 2002; Silva and Mooney 2010). Several previous studies using a bolus delivery method have demonstrated that doses of 10-30 ng/g resulted in increased neovascularisation *in vivo*. Other studies have shown that a lower dose of 4 ng/g of VEGF released from PLGA microparticles in an alginate gel was sufficient to induce angiogenesis *in vivo* (Lee and Lee 2009). The delivery system developed in this study is thus desirable since the kinetics achieved enabled the release of therapeutically relevant VEGF concentrations which may promote enhanced vasculogenesis (Pufe *et al.* 2002). Another critically important characteristic of the delivery system is its ability to maintain the bioactivity of the GF pre- and post-processing. The results demonstrated that VEGF released from the MPs enhanced tubule network formation by endothelial cells suggesting that alginate encapsulation provided protection to degradation from the acidic environment of the scaffold slurry and during the freezedrying process. Taken together, these encouraging results demonstrate that a fabrication process for scaffolds showing spatiotemporally controlled GF delivery was developed.

The functionalised scaffold was shown to enhance angiogenesis and bone regeneration in a critically sized rat calvarial defect model by 8 weeks post- implantation. Since angiogenesis involves the movement of ECs towards gradients of VEGF, it is likely that the scaffold sustained sufficient VEGF gradients across the scaffold-tissue interface to elicit an enhanced biological response *in vivo*. In addition to the number of vessels increasing, the size of the vessels was shown to increase in the VEGF-functionalised scaffold. It is likely that some of these large vessels were derived from newly formed capillaries resulting from increased vessel density in the VEGF-MP group. VEGF release from the material may have indirectly increased bone formation as a consequence of increasing blood flow in the defect site by laying down a supportive vascular network. Furthermore, the ability of VEGF to promote chemotaxis and differentiation of osteoblasts is known (Patel *et al.* 2008) and is

consistent with previous studies which showed that the release of VEGF from biomaterials can enhance bone regeneration in critical sized defects (Geiger *et al.* 2005; Kaigler *et al.* 2006; Clarke *et al.* 2007; Wernike *et al.* 2010). The potential of CHA scaffolds to promote mineralisation within a calvarial defect has previously been demonstrated. Histomorphometry revealed that functionalised scaffolds significantly enhanced bone repair compared to the non-VEGF eluting empty CHA scaffolds. The discrepancy between this result and the microCT analysis, which demonstrated a non-significant enhancement in bone volume in the functionalised scaffolds compared to the empty scaffold control, may be explained by the higher area of mature bone compared to earlier mineralised tissue in the microCT analysis. Nonetheless, this study has shown that controlled VEGF release led to increased vessel density and vessel size, accompanied by *de novo* bone formation and early bone healing of a critically sized bone defect.

The functionalised scaffolds described herein represent a promising approach for overcoming the associated problems of uncontrolled drug delivery for tissue engineering. Both the spray drying and the freeze-drying techniques, used for the fabrication of MPs and the scaffolds respectively are reproducible processes which can be easily scaled up to industrial production (I Ré 1998; George and Abraham 2006). Another potential avenue which could be explored is the adaptability of this pro-angiogenic material to a range of other applications to enhance vascularisation in ischemic tissues. Freeze-dried collagen-based scaffolds are currently being used for the regeneration of a wide range of tissues, such as cartilage (De Franceschi *et al.* 2005), cornea (Griffith *et al.* 2009) and blood vessels (Buttafoco *et al.* 2006). Thus, this system has an enormous potential in regenerative medicine, as it could be tuned in terms of the composition of the collagen-based scaffold and released therapeutic to be optimized for the healing of very diverse organs.

5. Conclusion

This study demonstrated the successful fabrication of a novel functionalised collagen-based scaffold capable of the spatiotemporal controlled release of VEGF through the incorporation of spray-dried alginate microparticles. The procedure for functionalising these scaffolds maintained VEGF bioactivity as it was proficient at increasing tubule formation by endothelial cells *in vitro*. These functionalised scaffolds were capable of sustaining the release of VEGF for up to 35 days. When implanted *in vivo* in a rat calvarial bone defect model this functionalised scaffold led to enhanced vessel formation after 8 weeks. In addition, the release of VEGF also resulted in increased bone regeneration. The process developed to functionalise these scaffolds, may offer an ideal platform to promote angiogenesis and tissue regeneration for a wide variety of applications in addition to bone.

6. Acknowledgements

Research in this publication was supported by the European Research Council grant 239685-CollRegen-ERC-2009-STG. A. L.-N. has been supported by Enterprise Ireland under project number CFTD/2009/0127 and Science Foundation Ireland under Grant SFI 12/TIDA/B2383. Peter O'Reilly Trinity College Dublin is acknowledged for his help with microCT. Michael McDonald and Prof. Veronica Campbell's lab in Trinity College Dublin are acknowledged for their help with confocal microscopy.

A

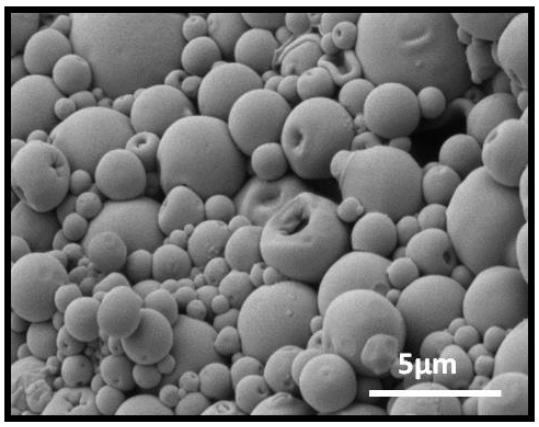
5µm

B

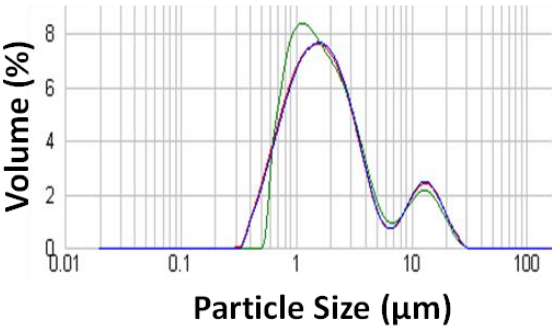
Volume (%)
8
6
4
2
0
0.01
0.1
1
10
100
Particle Size (µm)

C

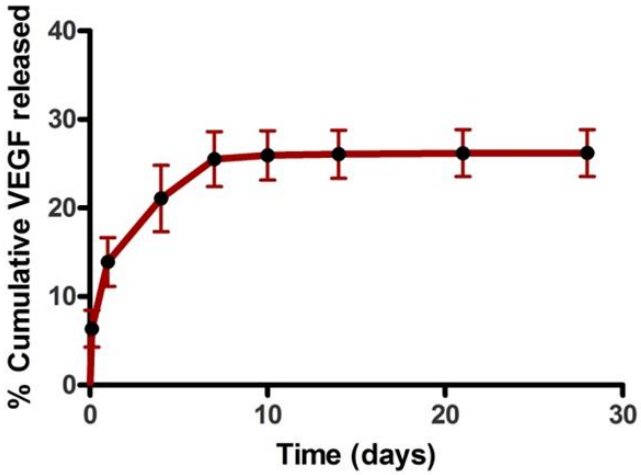
% Cumulative VEGF released
40
30
20
10
0
0
10
20
30
Time (days)

Figure. 1

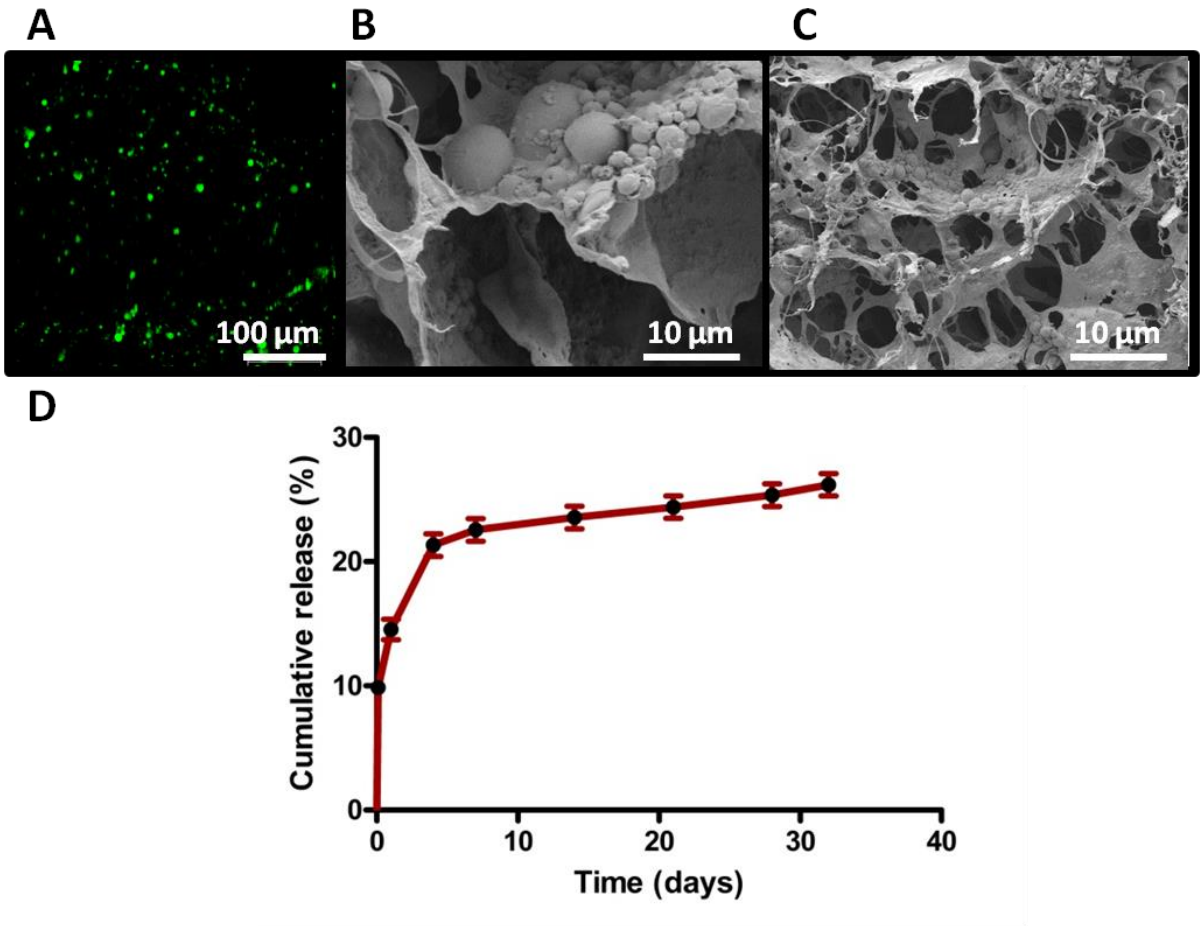
A
B
C
100 µm
10 µm
10 µm
D
Cumulative release (%)
30
20
10
0
0
10
20
30
40
Time (days)

Figure. 2

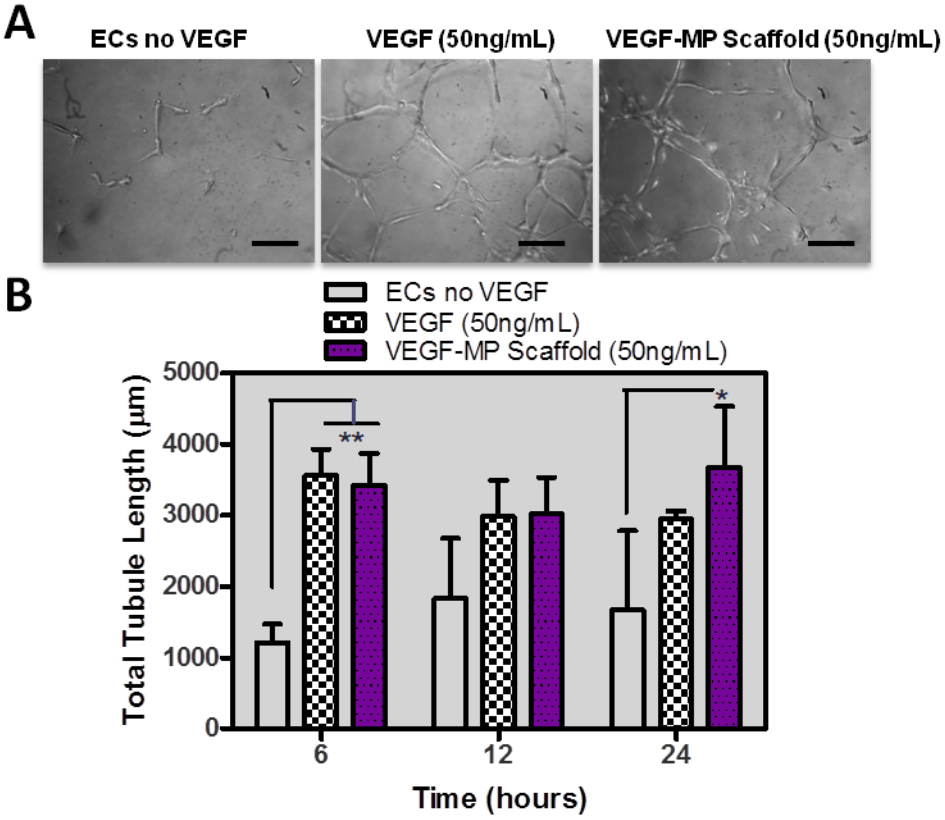
A
ECs no VEGF
VEGF (50ng/mL)
VEGF-MP Scaffold (50ng/mL)
B
ECs no VEGF
VEGF (50ng/mL)
VEGF-MP Scaffold (50ng/mL)
Total Tubule Length (µm)
5000
4000
3000
2000
1000
0
**
*
6
12
24
Time (hours)

Figure. 3

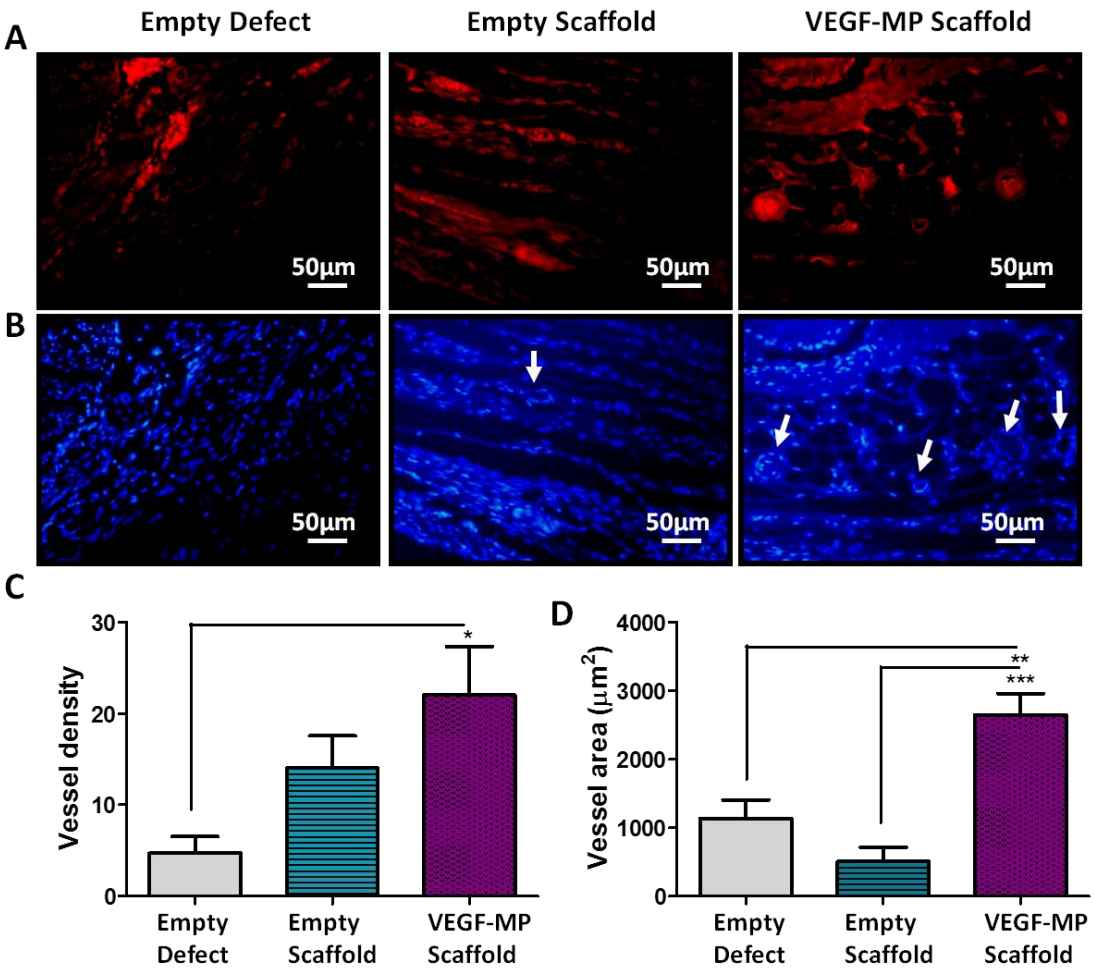
A
Empty Defect
Empty Scaffold
VEGF-MP Scaffold
50µm
B
C
Vessel density
30
20
10
0
*
Empty Defect
Empty Scaffold
VEGF-MP Scaffold
D
Vessel area (µm²)
4000
3000
2000
1000
0
**
***
Empty Defect
Empty Scaffold
VEGF-MP Scaffold

Figure. 4

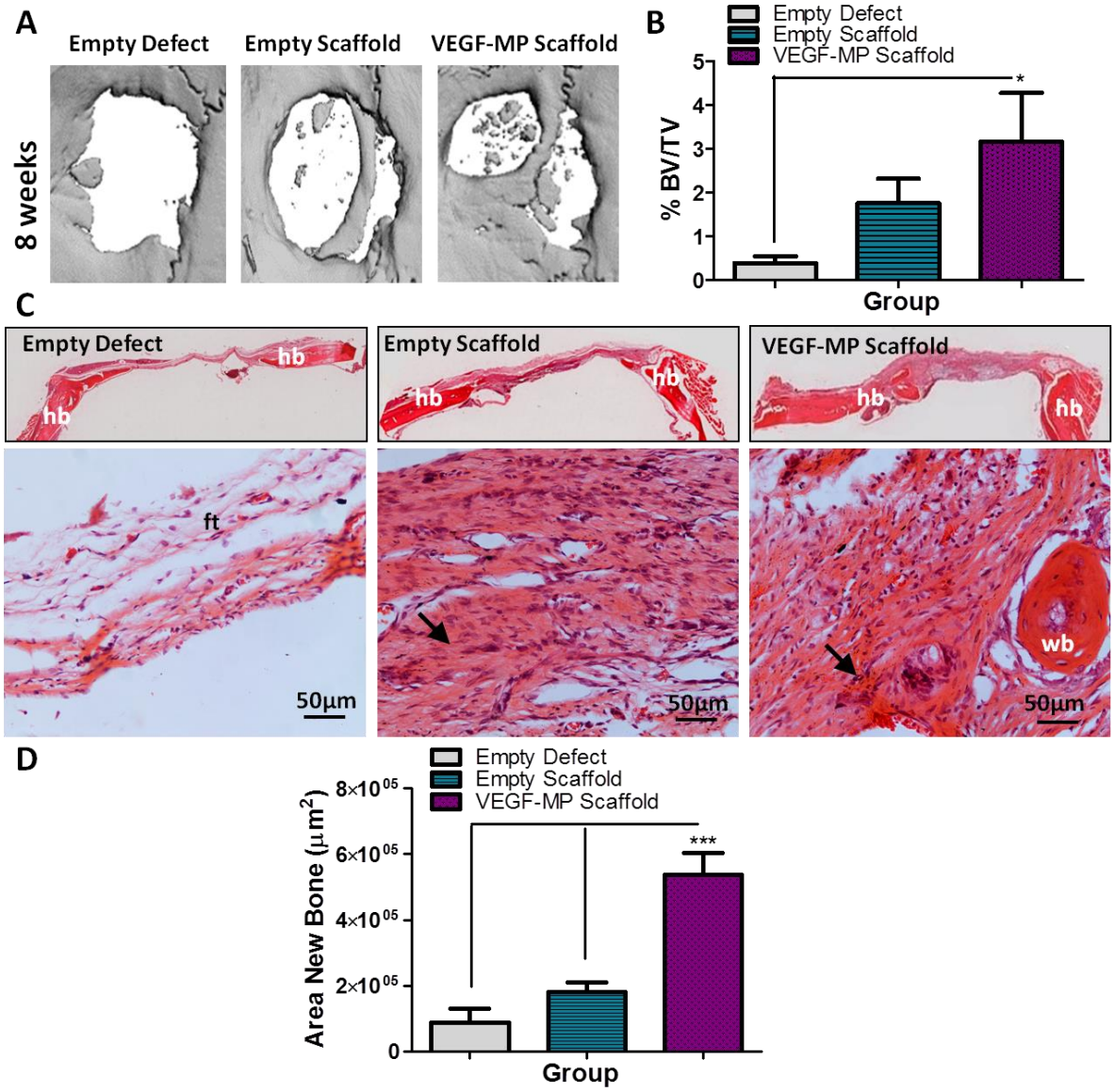

Figure. 5

References

Abramoff MD, Magelhaes PJ and Ram SJ (2004). "Image Processing with ImageJ." Biophotonics International **11**(7): 36-42.

Borselli C, Ungaro F, Oliviero O*, et al.* (2010). "Bioactivation of collagen matrices through sustained VEGF release from PLGA microspheres." J Biomed Mater Res A **92**(1): 94-102.

Bowey K, Swift BE, Flynn LE*, et al.* (2013). "Characterization of biologically active insulin-loaded alginate microparticles prepared by spray drying." Drug Dev Ind Pharm **39**(3): 457-465.

Buttafoco L, Engbers-Buijtenhuijs P, Poot AA*, et al.* (2006). "First steps towards tissue engineering of small-diameter blood vessels: preparation of flat scaffolds of collagen and elastin by means of freeze drying." J Biomed Mater Res B Appl Biomater **77**(2): 357-368.

Byrne EM, Farrell E, McMahon LA*, et al.* (2008). "Gene expression by marrow stromal cells in a porous collagen-glycosaminoglycan scaffold is affected by pore size and mechanical stimulation." J Mater Sci Mater Med **19**(11): 3455-3463.

Chen RR and Mooney DJ (2003). "Polymeric growth factor delivery strategies for tissue engineering." Pharm Res **20**(8): 1103-1112.
Clarke SA, Hoskins NL, Jordan GR*, et al.* (2007). "Healing of an ulnar defect using a proprietary TCP bone graft substitute, JAX, in association with autologous osteogenic cells and growth factors." Bone **40**(4): 939-947.
Cunniffe GM, Dickson GR, Partap S*, et al.* (2010). "Development and characterisation of a collagen nano-hydroxyapatite composite scaffold for bone tissue engineering." J Mater Sci Mater Med **21**(8): 2293-2298.
De Franceschi L, Grigolo B, Roseti L*, et al.* (2005). "Transplantation of chondrocytes seeded on collagen-based scaffold in cartilage defects in rabbits." J Biomed Mater Res A **75**(3): 612-622.
Epstein NE (2011). "Pros, cons, and costs of INFUSE in spinal surgery." Surg Neurol Int **2**: 10.
Geiger F, Bertram H, Berger I*, et al.* (2005). "Vascular endothelial growth factor gene-activated matrix (VEGF165-GAM) enhances osteogenesis and angiogenesis in large segmental bone defects." J Bone Miner Res **20**(11): 2028-2035.
George M and Abraham TE (2006). "Polyionic hydrocolloids for the intestinal delivery of protein drugs: alginate and chitosan--a review." J Control Release **114**(1): 1-14.
Gleeson JP, Plunkett NA and O'Brien FJ (2010). "Addition of hydroxyapatite improves stiffness, interconnectivity and osteogenic potential of a highly porous collagen-based scaffold for bone tissue regeneration." Eur Cell Mater **20**: 218-230.
Griffith M, Jackson WB, Lagali N*, et al.* (2009). "Artificial corneas: a regenerative medicine approach." Eye (Lond) **23**(10): 1985-1989.
Hascicek C, Gonul N and Erk N (2003). "Mucoadhesive microspheres containing gentamicin sulfate for nasal administration: preparation and in vitro characterization." Farmaco **58**(1): 11-16.
Haugh MG, Murphy CM and O'Brien FJ (2010). "Novel freeze-drying methods to produce a range of collagen-glycosaminoglycan scaffolds with tailored mean pore sizes." Tissue Eng Part C Methods **16**(5): 887-894.
Hulbert SF, Young FA, Mathews RS*, et al.* (1970). "Potential of ceramic materials as permanently implantable skeletal prostheses." J Biomed Mater Res **4**(3): 433-456.
I Ré M (1998). "Microencapsulation by spray drying." Drying Technology **16**(6): 1195-1236.
Kaigler D, Wang Z, Horger K*, et al.* (2006). "VEGF scaffolds enhance angiogenesis and bone regeneration in irradiated osseous defects." J Bone Miner Res **21**(5): 735-744.
Keogh MB, FJ OB and Daly JS (2010). "A novel collagen scaffold supports human osteogenesis--applications for bone tissue engineering." Cell Tissue Res **340**(1): 169-177.
Kubota Y, Kleinman HK, Martin GR*, et al.* (1988). "Role of laminin and basement membrane in the morphological differentiation of human endothelial cells into capillary-like structures." J Cell Biol **107**(4): 1589-1598.
Langer R (1998). "Drug delivery and targeting." Nature **392**(6679 Suppl): 5-10.
Lee J and Lee KY (2009). "Local and sustained vascular endothelial growth factor delivery for angiogenesis using an injectable system." Pharm Res **26**(7): 1739-1744.
Lee KY and Mooney DJ (2012). "Alginate: properties and biomedical applications." Prog Polym Sci **37**(1): 106-126.
Lieberman JR, Daluiski A and Einhorn TA (2002). "The role of growth factors in the repair of bone. Biology and clinical applications." J Bone Joint Surg Am **84-A**(6): 1032-1044.
Lu CH, Chang YH, Lin SY*, et al.* (2013). "Recent progresses in gene delivery-based bone tissue engineering." Biotechnol Adv **31**(8): 1695-1706.
Lyons FG, Gleeson JP, Partap S*, et al.* (2014). "Novel Microhydroxyapatite Particles in a Collagen Scaffold: A Bioactive Bone Void Filler?" Clinical Orthopaedics and Related Research®: 1-11.
Lyons FG, Al-Munajjed AA, Kieran SM*, et al.* (2010). "The healing of bony defects by cell-free collagen-based scaffolds compared to stem cell-seeded tissue engineered constructs." Biomaterials **31**(35): 9232-9243.

Marino JT and Ziran BH (2010). "Use of Solid and Cancellous Autologous Bone Graft for Fractures and Nonunions." Orthopedic Clinics of North America **41**(1): 15-26.
Mayr-Wohlfart U, Waltenberger J, Hausser H*, et al.* (2002). "Vascular endothelial growth factor stimulates chemotactic migration of primary human osteoblasts." Bone **30**(3): 472-477.
McCoy RJ, Widaa A, Watters KM*, et al.* (2013). "Orchestrating osteogenic differentiation of mesenchymal stem cells--identification of placental growth factor as a mechanosensitive gene with a pro-osteogenic role." Stem Cells **31**(11): 2420-2431.
Murphy CM and O'Brien FJ (2010). "Understanding the effect of mean pore size on cell activity in collagen-glycosaminoglycan scaffolds." Cell Adh Migr **4**(3): 377-381.
Norrby K and Ridell B (2003). "Tumour-type-specific capillary endothelial cell stainability in malignant B-cell lymphomas using antibodies against CD31, CD34 and Factor VIII." APMIS **111**(4): 483-489.
Novosel EC, Kleinhans C and Kluger PJ (2011). "Vascularization is the key challenge in tissue engineering." Adv Drug Deliv Rev **63**(4-5): 300-311.
O'Brien FJ, Harley BA, Yannas IV*, et al.* (2005). "The effect of pore size on cell adhesion in collagen-GAG scaffolds." Biomaterials **26**(4): 433-441.
O'Brien FJ, Lopez-Noriega A, Quinlan E*, et al.* (2012). A composite scaffold for use as a tissue engineering implant. Royal College of Surgeons in Ireland, P10963GB00.
O'Brien FJ, Gleeson, J. Plunkett, N (2008). A collagen/hydroxyapatite composite scaffold, and process for the production thereof. Royal College of Surgeons in Ireland, WO/2008/096334.
Patel ZS, Young S, Tabata Y*, et al.* (2008). "Dual delivery of an angiogenic and an osteogenic growth factor for bone regeneration in a critical size defect model." Bone **43**(5): 931-940.
Peters MC, Isenberg BC, Rowley JA*, et al.* (1998). "Release from alginate enhances the biological activity of vascular endothelial growth factor." J Biomater Sci Polym Ed **9**(12): 1267-1278.
Pufe T, Wildemann B, Petersen W*, et al.* (2002). "Quantitative measurement of the splice variants 120 and 164 of the angiogenic peptide vascular endothelial growth factor in the time flow of fracture healing: a study in the rat." Cell Tissue Res **309**(3): 387-392.
Quinlan E, Lopez-Noriega A, Thompson E*, et al.* (2015). "Development of collagen-hydroxyapatite scaffolds incorporating PLGA and alginate microparticles for the controlled delivery of rhBMP-2 for bone tissue engineering." J Control Release **198**: 71-79.
Reis CP, Neufeld RJ, Vilela S*, et al.* (2006). "Review and current status of emulsion/dispersion technology using an internal gelation process for the design of alginate particles." J Microencapsul **23**(3): 245-257.
Richardson TP, Peters MC, Ennett AB*, et al.* (2001). "Polymeric system for dual growth factor delivery." Nat Biotechnol **19**(11): 1029-1034.
Schoubben A, Blasi P, Giovagnoli S*, et al.* (2010). "Development of a scalable procedure for fine calcium alginate particle preparation." Chemical Engineering Journal **160**(1): 363-369.
Silva EA and Mooney DJ (2010). "Effects of VEGF temporal and spatial presentation on angiogenesis." Biomaterials **31**(6): 1235-1241.
Sivadas N, O'Rourke D, Tobin A*, et al.* (2008). "A comparative study of a range of polymeric microspheres as potential carriers for the inhalation of proteins." Int J Pharm **358**(1-2): 159-167.
Stacker SA and Achen MG (1999). "The vascular endothelial growth factor family: signalling for vascular development." Growth Factors **17**(1): 1-11.
Street J, Bao M, deGuzman L*, et al.* (2002). "Vascular endothelial growth factor stimulates bone repair by promoting angiogenesis and bone turnover." Proc Natl Acad Sci U S A **99**(15): 9656-9661.
Suehiro J, Hamakubo T, Kodama T*, et al.* (2010). "Vascular endothelial growth factor activation of endothelial cells is mediated by early growth response-3." Blood **115**(12): 2520-2532.

Swetha M, Sahithi K, Moorthi A*, et al.* (2010). "Biocomposites containing natural polymers and hydroxyapatite for bone tissue engineering." International Journal of Biological Macromolecules **47**(1): 1-4.
Tsiridis E, Upadhyay N and Giannoudis P (2007). "Molecular aspects of fracture healing: which are the important molecules?" Injury **38 Suppl 1**: S11-25.
Vehring R (2008). "Pharmaceutical particle engineering via spray drying." Pharmaceutical Research **25**(5): 999-1022.
Wahl DA and Czernuszka JT (2006). "Collagen-hydroxyapatite composites for hard tissue repair." Eur Cell Mater **11**: 43-56.
Weadock KS, Miller EJ, Keuffel EL*, et al.* (1996). "Effect of physical crosslinking methods on collagen-fiber durability in proteolytic solutions." J Biomed Mater Res **32**(2): 221-226.
Weadock KS, Miller EJ, Bellincampi LD*, et al.* (1995). "Physical crosslinking of collagen fibers: Comparison of ultraviolet irradiation and dehydrothermal treatment." J Biomed Mater Res **29**(11): 1373-1379.
Wernike E, Montjovent MO, Liu Y*, et al.* (2010). "VEGF incorporated into calcium phosphate ceramics promotes vascularisation and bone formation in vivo." Eur Cell Mater **19**: 30-40.
Zocchi MR, Ferrero E, Leone BE*, et al.* (1996). "CD31/PECAM-1-driven chemokine-independent transmigration of human T lymphocytes." Eur J Immunol **26**(4): 759-767.

Fig. 1 Microparticle characterisation. **(A)** Scanning electron micrograph of VEGF-MPs prepared by the spraydrying method showing particle sizes <10µm. Scale bars, 10 µm. **(B)** Microparticle size distribution indicating particle diameters in the range of <10 µm. **(C)** Cumulative VEGF release from alginate MPs.

Fig. 2 Microparticle scaffold composition and VEGF release. **(A)** Confocal image of alginate microparticles encapsulating BSA-FITC in a scaffold. Scale bar, 100 µm. **(B)** Scanning electron micrographs of surface and **(C)** cross sections of scaffolds incorporating 0.5% w/v alginate VEGF microparticles (1.6 µg of VEGF). Scale bars, 10 µm. **(D)** Cumulative VEGF release from VEGF-MP scaffolds over 35 days.

Fig. 3 Bioactivity of VEGF released from VEGF-MP scaffold in a tubule formation assay. **(A)** Microscopy images depicting tubule formation after 6 h in culture demonstrating enhanced tubule formation in the VEGF released from VEGF-MP scaffold groups. Scale

bars, 100 µm. **(B)** Quantification of tubule formation corroborating images taken at 6 h. ** $p<0.01$; * $p<0.05$ *vs* no VEGF control.

Fig. 4 Immunohistochemical analysis of vascular network formation. **(A)** CD31 labelled endothelial cells and **(B)** DAPI stained nuclei in sections of empty defect, empty scaffold and VEGF-MP scaffolds indicating enhanced vessel density (white arrow) in VEGF-MP groups compared to the controls at 8 weeks. Scale bars, 50 µm. **(C)** Vessel density in implants indicating an increase in the VEGF-MP group compared to the empty defect (* $p<0.05$) and empty scaffold. **(D)** Total area of new vessel formation indicating an increase in the VEGF-MP group compared the empty defect (** $p<0.01$) and empty scaffold (*** $p<0.001$). One-way ANOVA and post-hoc Tukey post-test performed.

Fig. 5 Microcomputed tomographical analysis and histomorphometrical analysis of explants demonstrating the level of bone repair. **(A)** Qualitative and **(B)** quantitative microcomputed tomographical analysis of empty defect, empty scaffold and VEGF-MP scaffolds at 8 weeks post-implantation demonstrating that the VEGF-MP group supported the highest level of bone formation compared to empty defect (** $p<0.01$) and empty scaffold (* $p<0.05$). One-way ANOVA and post-hoc Tukey post-test performed. **(C)** Haematoxylin and eosin stained sections of empty defect, empty scaffold and VEGF-MP scaffolds showing the full specimen with the original host bone (hb) (top panels). Fibrotic tissue (ft) is visible in the empty defect while a layer of bone formation with mineralised tissue (black arrows) is visible in the empty scaffold and a dense layer of bone formation is seen in the VEGF-MP group with woven bone (wb) visible (bottom panels at 20x mag). Scale bars, 50 µm. **(D)** Quantitative histomorphometric analysis indicating the mean total area of bone nucleation sites and accelerated bone healing in VEGF-MP scaffolds compared to empty scaffolds and empty

defect (*** p<0.001). One-way ANOVA and Dunns Multiple Comparison post-test performed.